Sub-Wavelength Anisotropic Unit-Cells for Low-Profile Transmitarray Antennas

Andrea Tummolo, Orestis Koutsos, Francesco Foglia Manzillo, Antonio Clemente, Agnese Mazzinghi, Angelo Freni, Ronan Sauleau

Sub-Wavelength Anisotropic Unit-Cells for Low-Profile Transmitarray Antennas

Andrea Tummolo[1], Orestis Koutsos[1], Francesco Foglia Manzillo[2], Antonio Clemente[2], Agnese Mazzinghi[3], Angelo Freni[3], Ronan Sauleau[1]

[1] Univ Rennes, CNRS, IETR – UMR 6164, F-35000 Rennes, France ({andrea.tummolo,orestis.koutsos, ronan.sauleau}@univ-rennes.fr)

[2] CEA-Leti, Univ. Grenoble-Alpes, F-38054 Grenoble, France ({francesco.fogliamanzillo, antonio.clemente}@cea.fr)

[3] University of Florence, 50139 Florence, Italy ({agnese.mazzinghi, angelo.freni}@unifi.it)

***Abstract*— This paper presents the design of a sub-wavelength (sub-WL) element with anisotropic properties and demonstrates the performance enhancement it offers for realizing low-profile transmitarrays. The transmission characteristics are analyzed and compared to those of similar half-wavelength (half-WL) elements. The results reveal that, as opposed to the half-wavelength cell, the sub-wavelength element exhibits minimal sensitivity to oblique incidence effects, a key issue for low-profile transmitarrays. To evaluate the impact of the angular robustness of the element on the transmitarray performance, four distinct prototypes with 3-bit phase resolution and 10×10 λ^2 size, featuring the two unit-cell types and two different focal-to-diameter ratios (*F/D* = 0.85, 0.3) are designed at 30 GHz. The low-profile antenna with sub-wavelength elements attains a peak gain of 28.1 dBi with 46% aperture efficiency and a −3-dB gain bandwidth of 35%, outperforming the transmitarray based on half-wavelength elements.**

Keywords—low-profile, oblique incidence, sub-wavelength unit-cell, transmitarray antennas.

I. Introduction

Over the past few years, transmitarray (TA) antennas have attracted wide interest in the development of low-cost and high-gain radiating systems at millimeter-wave frequencies. They consist of planar discrete lenses that convert the beam shape of the incident field, typically emitted by a low- or moderate-gain feeding source, into a desired far- or near-field pattern through a proper phase compensation. TA antennas benefit from the spatial feeding mechanism, which avoids potentially significant losses associated with beam-forming networks, as in the case of phased arrays. However, the focal length *F* between the primary source and the TA aperture may be a drawback for some applications with strict constraints on the antenna volume, especially at frequencies lower than Ka-band frequencies. Consequently, one of the critical challenges in designing TA antennas is to reduce their focal-to-diameter ratio (*F/D*) while maintaining high efficiency and large bandwidth. This critical pursuit has prompted a multitude of innovative techniques and methodologies within the existing literature. These methods encompass several strategies, such as the optimization of the antenna feed [1], [2], folded structures [3], [4], and tailoring the phase profile [5]. Nevertheless, as we delve deeper into the challenges of profile reduction, an essential consideration emerges about the impact of oblique incidence, regardless of the solution employed to reach this goal.

To achieve the desired transmission characteristics, the TA elements are generally optimized as unit-cells (UCs) of infinite periodic structures, normally illuminated by an incident plane wave. Therefore, the elements are placed accurately within the TA lattice to produce the desired phase compensation. This approach is valid under the hypothesis that the magnitude and phase responses of these UCs remain unaffected by the angle of incidence of the incoming wave. While this assumption holds within a reasonably small error for center-fed TAs with sufficiently large *F/D* ratios, it becomes increasingly inaccurate as we move toward low-profile configurations. For example, the work in [6] demonstrated that designing a TA (*F/D* = 0.8) neglecting the variation of the transmission coefficients of the UCs can lead up to a 5 dB gain drop at the design frequency, compared to the actual case that takes into account the oblique incidence angles. Furthermore, in [7], a method based on generating the phase profile of a dielectric TA considering the oblique incidence effect is introduced. This approach results in a remarkable gain enhancement of 4.5 dB for a highly compact configuration (*F/D* = 0.14).

The previous studies underscore the importance of exploring new design solutions at the UC level to create elements that exhibit minimal sensitivity to oblique incidence. Over the past two decades, various element designs have been presented. Designs based on symmetrical frequency-selective-surfaces (FSSs) require at least four metal layers to cover the 360° phase range and simultaneously achieve –1-dB transmission [8]. However,

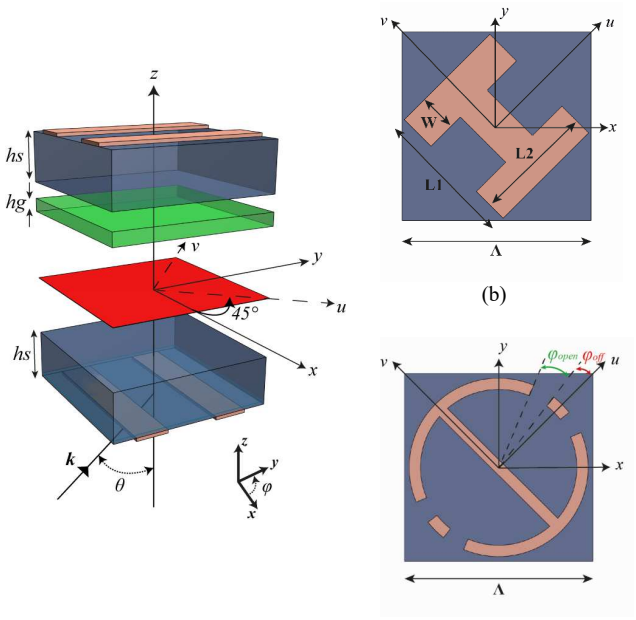

Fig. 1. (a) Exploded view of the anisotropic unit-cell. In the rotator layer (in red), the coordinate system (CS) transformation from the reference CS *(x,y)* to the crystal CS *(u,v)* is illustrated. Rotator geometries employed for (b) the half-WL (c) and sub-WL configurations. The periodic size *Λ* is 5 mm and 2 mm, respectively.

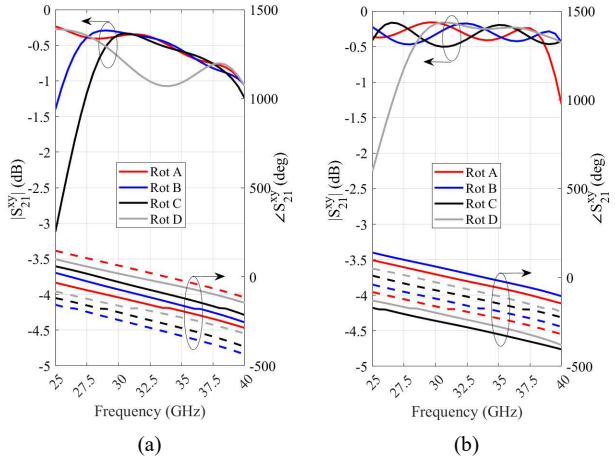

Fig. 2. Simulated transmission magnitude and phase of the half-WL UC (a) and sub-WL UC (b). The dashed lines refer to the transmission phase of the mirrored cases.

TABLE I

GEOMETRICAL PARAMETERS OF THE ROTATORS FOR THE HALF-WL UNIT-CELL

Rotator	L1 (mm)	W (mm)	L2 (mm)
A	3.7	1	3.2
B	3.5	1	2.55
C	3.3	1.2	2.1
D	3.3	1.5	1.4

TABLE III

GEOMETRICAL PARAMETERS OF THE ROTATORS FOR THE SUB-WL UNIT-CELL

Rotator	φ_{op} (deg)	φ_{off} (deg)
A	15	7
B	25	10
C	30	16.5
D	20	41

aiming to realize a low-profile structure, thin elements with a minimum number of metal layers are required. In [9], an asymmetric UC design is introduced. Thanks to the anisotropic properties of this element, complete phase coverage and a near-perfect transmission can be achieved using only three metal layers. Nevertheless, in the pursuit of low-profile configurations, the selected UC shall also exhibit minimal sensitivity to oblique incidence. Existing literature indicates that periodicity can enhance the antenna bandwidth [10]. In this context, this contribution discusses the impact of periodicity on the UC angular robustness.

In section II, we present a comparison between two UC designs based on the same architecture but exhibiting different square lattice sizes. Their transmitting performance at the UC level is numerically analyzed for both normal and oblique incidence. Our results demonstrate the remarkable insensitivity of the sub-WL UC to the variation of the incidence direction. In section III, in order to investigate the impact of the UC angular robustness on the TA performance,

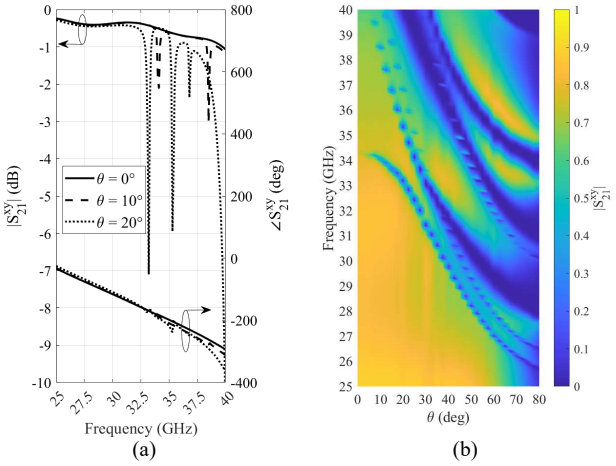

Fig. 3. Half-WL UC (Rotator A): (a) Transmission magnitude and phase for different angles of incidence. (b) Transmission magnitude as a function of both frequency and incidence angle.

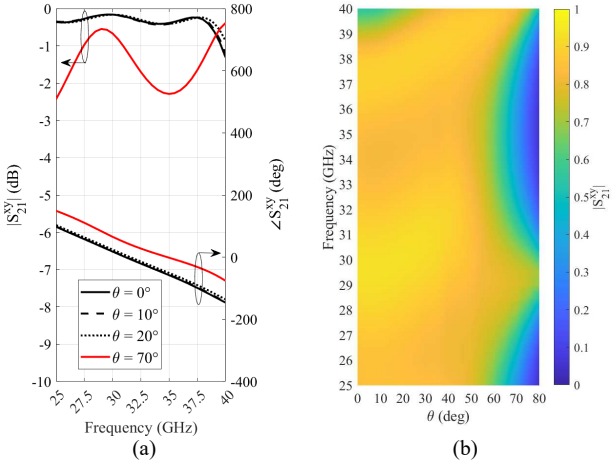

Fig. 4. Sub-WL UC (Rotator A): (a) Transmission magnitude and phase for different angles of incidence. (b) Transmission magnitude as a function of both frequency and incidence angle.

multiple TA antennas based on the two proposed UCs are analyzed by considering a standard-profile (F/D = 0.85) and low-profile configurations (F/D = 0.3).

II. UNIT-CELL DESIGN

A schematic representation of the UC is depicted in Fig. 1(a). It comprises three metal layers and two dielectric substrates, held together using a bonding film. The outer layers consist of orthogonal metallic strip gratings, serving as linear polarizers. These two gratings share identical dimensions, differing only in the orientation of their strips. The inner layer, referred to as the rotator, comprises a dipole-like element tilted by 45° with respect to the *xy*-system. The UC leverages the multiple reflections within the cavity and the anisotropic properties of the rotator to gradually convert the polarization of the incoming wave, simultaneously introducing the desired phase shift. Complete tuning of the phase shift with near-zero insertion loss can be achieved by only adjusting the dimensions of the inner element; 4 different rotator geometries have been considered (Rot A, Rot B, Rot C, and Rot D). Moreover, a 180° phase shift can be obtained by simply mirroring each rotator, streamlining the design process, thus leading to 8 different rotators, i.e. a 3-bit phase

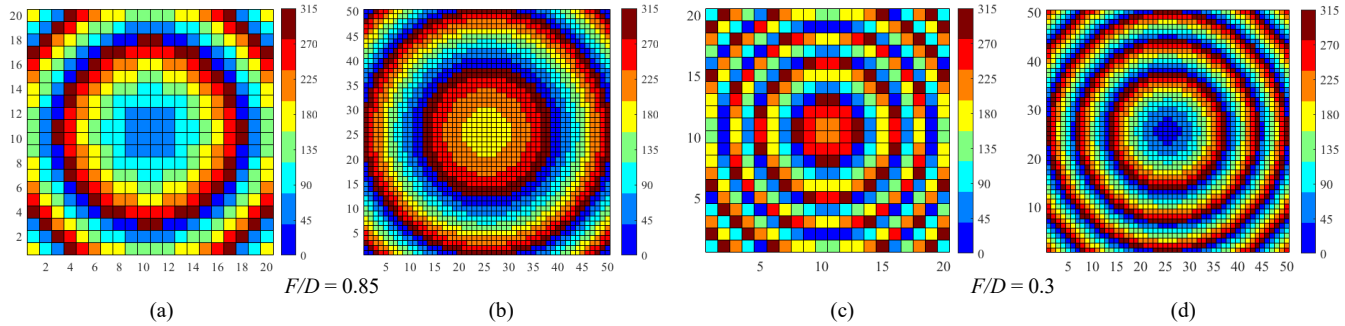

Fig. 5. Phase profiles of the half-WL (a), (c) and sub-WL (b), (d) TAs for different values of *F/D*. They are calculated at 30 GHz to steer the beam at the broadside.

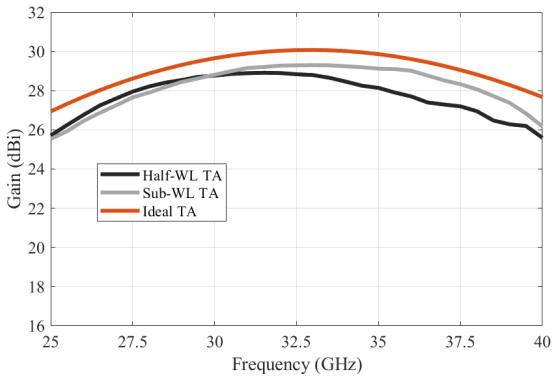

Fig. 6. Simulated peak gain as a function of frequency of the half-WL and sub-WL TAs for F/D = 0.85. Comparison with an ideal TA.

resolution. A comprehensive numerical model and design procedure for this UC are described in [9].

The following Sections II.A and II.B present two different UC designs with distinct periodic sizes. The first structure, referred to as half-WL UC, has a period of $\lambda/2 \times \lambda/2$, where λ is the wavelength in the free space at 30 GHz. In the second one, referred to as sub-WL UC, the periodicity is set to $\lambda/5$.

A. Half-WL Unit-Cell

The first proposed UC has a size of 5×5 mm^2. The substrate material is a low-permittivity Duroid 5880 (ε_r= 2.2, $\tan\delta = 0.9 \times 10^{-3}$), while the bonding film is made of Arlon CuClad 6700 ε_r= 2.35, $\tan\delta = 2.5 \times 10^{-3}$). The thicknesses are set to $h_s = 1.575$ mm and $h_g = 40$ µm for the dielectric and bonding layers, respectively. The polarizers consist of strips with a width of 0.9 mm and center-to-center spacing of 1.75 mm.

In accordance with the design guidelines, the rotator shall exhibit purely capacitive and inductive properties for each polarization in the *(u,v)* coordinate system (CS) to maximize the transmission magnitude. Following the design procedure explained in [9], an I-shape dipole is constructed, as shown in Fig. 1(b). By adjusting the length of both the dipole, L1, and of the hats, L2, as well their widths, W, four different phase states are optimized. Moreover, four additional states are also obtained by mirroring the rotator with respect to the *y*-axis, resulting in a 3-bit phase resolution. The physical dimensions of the rotator configurations are provided in Table I.

Fig. 2 (a) shows the simulated transmission magnitude and phase of these UCs for normal incidence and enforcing periodic boundary conditions. Each UC covers at least 11.3 GHz (37%) of -1-dB transmission bandwidth. The relative phase error is less than 2° between adjacent UC phase responses at the design frequency and becomes larger at higher frequencies.

Lastly, the transmission performance of the UC is investigated for several oblique incidence angles of the incoming wave. The performance in transmission magnitude and phase for different angles of incidence in the E-plane is shown in Fig. 3(a). It can be seen that the selected UC exhibits a stable performance for angles lower than 20º and up to 33 GHz. However, the frequency responses deteriorate rapidly for larger angles and becomes worse at higher frequencies. This effect is a result of the selected periodicity of the inner layer, which leads to the onset of trapped higher-order grating modes[11]. Fig. 3 (b) depicts the magnitude of the transmission coefficient of one of the half-wave UCs as a function of both frequency and incidence angle. Its degradation becomes even more evident for larger incidence angles.

B. Sub-WL Unit-Cell

The sub-WL element, shown in Fig. 1(c), has a periodicity $\Lambda = 2$ mm ($\lambda/5$ at 30 GHz). It features dielectric spacers made of Duroid 6002 (ε_r= 2.94, $\tan\delta = 1.2 * 10^{-3}$) with a thickness of $h_s = 1.524$ mm and employs the same bolding film as for the previous case. In this configuration, the strip width and spacing of the polarizing grids are equal to 0.45 mm and 0.6 mm, respectively.

Following the same design approach, a new rotator shape is introduced to reach the maximum performance for the selected periodic size. In this case, the proposed structure combines a dipole and a circular ring with four cuts (Fig. 1(c)). The dipole length is set to $2R = 1.9$ mm. The transmission phase is tuned by changing the angles φ_{op} and φ_{off}, which govern the widths and positions of four identical and symmetrical cuts on the ring. The values of φ_{op} and φ_{off} are optimized for a 3-bit phase resolution and listed in Table II.

The transmission magnitude and phase are plotted in Fig. 2(b). All UCs cover more than 40% of fractional bandwidth with losses better than 0.5 dB over the entire region of interest. The phase error remains stable and is less than 10° over the frequency range of 25-40 GHz. The operating bandwidth is thus broader than that of the half-WL UC.

The performance enhancement enabled by the sub-WL UC compared to the half-WL is even clearer when considering the response under oblique incidence. Thanks to its smaller periodic size, the structure is less affected by variations in the incidence direction, as demonstrated in Fig. 4(a). Specifically, the magnitude of the transmission coefficient remains above 3 dB for incidence angles up to 70º over the entire frequency region. Although the transmission phase slightly varies, the phase slope as a function of frequency remains similar to that obtained for normal incidence. Finally, in contrast to the

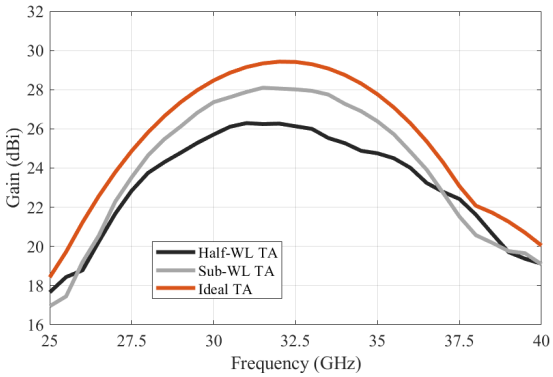

Fig. 7. Simulated gain frequency response of the two prototypes with an F/D = 0.3, based on half-WL and sub-WL UCs, compared to an ideal (perfectly collimating and lossless) TA.

previous case, no resonant points can be found, as can be seen in Fig. 4(b). Based on these results, the sub-WL UC can enable a more efficient design of TAs with very low profiles.

III. Transmitarray Design

To assess the performance of low-profile TAs based on the two proposed UC types, several designs are numerically studied. Specifically, for each UC design, two TAs are synthesized at 30 GHz: one with a relatively large F/D = 0.85, and one with a small F/D = 0.3. It leads to four different antenna systems. Two different ideal sources, modeled using cosine-type radiation patterns, are selected for the two considered F/D values. Both setups provide the maximum achievable gain for the employed illumination. Specifically, the gain of the source is described as $G_{FS} = (n+1)\cos^n\theta$, where n defines the peak gain and the half-power beamwidth (HPBW) [12]. For the standard-profile designs (F/D = 0.85), n is set to 15, whereas for the low-profile designs (F/D = 0.3), it is set to 1. In both cases, the edge taper of the TA is around –11 dB. The study and design of each TA are done using an *ad-hoc* numerical tool based on ray tracing, as reported in [13].

For all cases, the TA size is set to $10\lambda \times 10\lambda$ at 30 GHz, corresponding to 20×20 elements and 50×50 elements for the half-WL and the sub-WL designs, respectively.

A. Standard-Profile Transmitarray Antenna

The phase profiles of the half-WL and sub-WL TAs, numerically optimized at 30 GHz for broadside radiation with F/D = 0.85, are represented in Fig. 5(a) and (b). In both systems, the maximum illumination angle from the source is ±30º at the edge of the aperture.

Full-wave simulations using Ansys HFSS have been performed to validate the analysis of the proposed half-WL and sub-WL TAs. The cosine-shaped illumination is imposed by placing an external far field located in the focal point of the TA (i.e., at 85 mm from the TA surface). Their gain curves are shown in Fig. 6. Both designs achieve a gain of 28.8 dBi at the design frequency. When compared to an ideal TA, i.e., a lossless ideal lens providing perfect phase compensation, the sub-WL TA exhibits an almost constant gain loss of 0.8 dBi over the frequency region 25-40 GHz. The half-WL TA exhibits a slight gain decrease (~1.2 dB) at higher frequencies, which is due to the performance of the UC at oblique angles of illumination. Finally, the aperture efficiency is 61% for

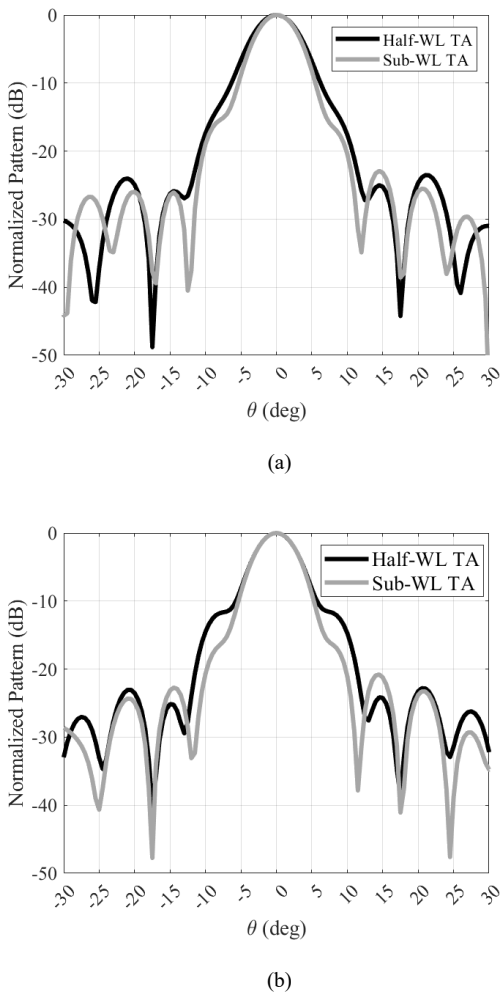

Fig. 8. Comparison between the simulated co-polarized radiation patterns of the half-WL and sub-WL TAs in the low-profile configuration (F/D = 0.3) at 30 GHz. (a) H-plane (b) and E-plane cut.

both configurations, resulting in comparable radiation performance.

B. Low-Profile Transmitarray Antenna

The phase profiles of the low-profile half-WL and sub-WL TAs for this setup (F/D = 0.3) are shown in Fig. 5(c) and (d).

The peak gain as a function of frequency is shown in Fig. 7. Unlike the standard-profile design, a notable difference in performance between the two TAs can be seen. Specifically, the half-WL TA exhibits a gain loss up of to 3.1 dB compared to the ideal TA, whereas the sub-WL TA exhibits only 1.1 dB of loss and reaches a peak gain of 28.1 dBi at 31.5 GHz. Hence, the maximum aperture efficiency is 46% and 32% at 31 GHz for the sub-WL and half-WL TAs, respectively, resulting in a better collimation capability by the TA with sub-WL cells. These divergent results can be attributed to two factors, both stemming from the choice of the UC periodicity. Firstly, in the proposed low-profile design, the angle of incidence can exceed 60° at the edges of the aperture, resulting in a relevant alteration to the scattering parameters of the UCs. However, thanks to the significant robustness of the smaller UCs to the impact of the oblique incidence, the sub-WL TA displays a limited degradation in performance compared to the half-WL design, confirming the results presented in Section II. Additionally, a low-profile

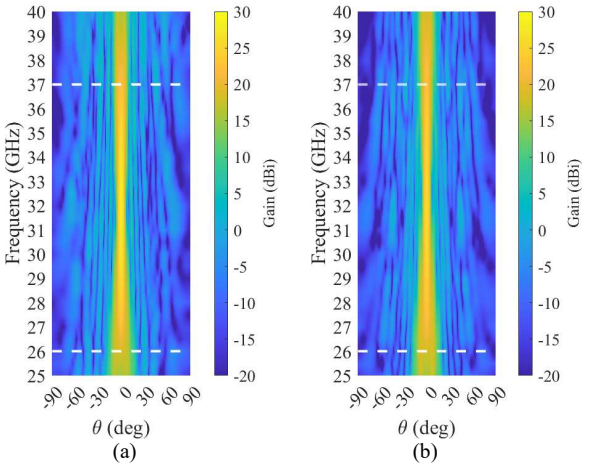

Fig. 9. Simulated co-polarized gain as a function of both frequency and elevation angle of the low-profile sub-wavelength TA ($F/D = 0.3$). (a) H-plane and (b) E-plane.

configuration demands a greater number of repetitions of full-phase circles (360°) on the phase distribution of the arrays, as can be observed in Fig. 5(c) and (d). Thanks to the smaller periodicity, the phase profile of the sub-WL TA is spatially smoother and avoids sudden phase shifts as in the case of the half-WL TA. It leads to a more effective phase compensation.

Furthermore, due to the broader bandwidth behavior of the smaller elements, the −3-dB gain bandwidth is 35% and 26% for the sub-WL and half-WL designs, respectively. Finally, the normalized radiation patterns at the design frequency of 30 GHz are compared for both orthogonal planes in Fig. 8(a) and (b). In the plots, the observed elevation angle is limited in the [-30°, 30°] range, revealing a narrower beam shape for the sub-WL TA. Moreover, the co-polarized gain of the sub-WL TA as a function of the elevation angle and frequency is depicted in Fig. 8. The main lobe is very stable in the −3-dB gain bandwidth, ensuring efficient beam collimation within the range of 26-37 GHz.

IV. Conclusion

An anisotropic TA design with λ/5 periodicity at 30 GHz was presented. The proposed three-layer sub-wavelength unit-cells can achieve nearly zero insertion loss and broadband transmission for normal incidence. A comprehensive analysis of the transmission performance for oblique incidence was conducted, showing significant angular robustness. To demonstrate the remarkable performance and the stability of this unit-cell design even for large angles, a 3-bit 50×50-element TA antenna was designed and optimized for $F/D = 0.3$. A peak gain of 28.1 dBi with 46% aperture efficiency and highly efficient focalization in a relatively large bandwidth was achieved. To quantitively analyze the benefit of the unit-cell robustness to oblique incidence on the TA performance, a TA with the same values of F, D, and source was designed using half-wavelength anisotropic elements similar to the previous ones. It emerges that the new sub-wavelength elements can improve the transmission performance (+14%) and bandwidth (+9%) of TAs with a small focal-to-diameter ratio, thereby paving the way for the realization of efficient low-profile discrete lenses.

Acknowledgment

This work has been partly supported by the OPALE project funded by “Ministère des Armées”, with the support of AID (Agence de l’Innovation de Défense), France.

References

[1] A. Clemente, L. Dussopt, R. Sauleau, P. Potier, and P. Pouliguen, "Focal distance reduction of transmit-array antennas using multiple feeds," *IEEE Antennas and Wireless Propag. Letters,* vol. 11, pp. 1311–1314, 2012.

[2] P.-Y. Feng, S. -W. Qu, S. Yang, L. Shen and J. Zhao, "Ku-Band Transmitarrays With Improved Feed Mechanism," *IEEE Trans. Antennas Propag.,* vol. 66, no. 6, pp. 2883-2891, Jun. 2018.

[3] Y. Ge, C. Lin, and Y. Liu, "Broadband folded transmitarray antenna based on an ultrathin transmission polarizer," *IEEE Trans. Antennas Propag.,* vol. 6, no. 11, p. 5974–5981, Nov 2018.

[4] C. Fan, W. Che, W. Yang, and S. He, "A novel PRAMC-based ultralow-profile transmitarray antenna by using ray tracing principle," *IEEE Trans. Antennas Propag.,* vol. 35, no. 4, p. 1779–1787, Apr. 2017.

[5] S. Matos et al, "Achieving wide-angle mechanical beam steering in Ka-band with low-profile transmit-array antennas," *2023 17th European Conference on Antennas and Propagation (EuCAP), Florence, Italy,* pp. 1-5, 2023.

[6] A. H. Abdelrahman, A. Z. Elsherbeni and F. Yang, "Transmitarray antenna design using cross-slot elements with no dielectric substrate," *IEEE Antennas Wirel. Propag. Lett.,* vol. 13, pp. 177-180, 2014.

[7] Y. Cai, P. Mei, X. Q. Lin and S. Zhang, "A generalized method for gain bandwidth enhancement of transmitarray antennas considering oblique incidences," *IEEE Trans. Circuits and Systems II: Express Briefs,* 2023.

[8] A. H. Abdelrahman, A. Z. Elsherbeni and F. Yang, "Transmission phase limit of multilayer frequency-selective surfaces for transmitarray designs," *IEEE Trans. Antennas Propag.,* vol. 62, no. 2, pp. 690-697, Feb. 2014.

[9] O. Koutsos, F. F. Manzillo, A. Clemente, and R. Sauleau, "Analysis, rigorous design, and characterization of a three-layer anisotropic transmitarray at 300 GHz," *IEEE Transactions on Antennas and Propagation,* vol. 70, no. 7, p. 5437–5446, Jul. 2022.

[10] D.M. Pozar, "Wideband reflectarrays using artificial impedance surfaces," *Electronics Letters,* vol. 43, no. 3, pp. 148 - 149, Feb. 2007.

[11] B.-A. Munk, Frequency Selective Surfaces - Theory and design, John Wiley & Sons, 2000.

[12] P.-S. Kildal, Foundations of antenna engineering: a unified approach for line-of-sight and multipath, Artrch, 2015.

[13] H. Kaouach, L. Dussopt, J. Lanteri, T. Koleck and R. Sauleau, "Wideband low-loss linear and circular polarization transmit-arrays in V-Band," *IEEE Trans. Antennas Propag.,* vol. 59, no. 7, pp. pp. 2513-2523, July 2011.